Journal of Civil Engineering and Construction 2025;14(3):126-135
https://doi.org/10.32732/jcec.2025.14.3.126

Evaluating the Effect of Welding Defect on Seismic Collapse Capacity of Steel Moment Resisting Frames

Kourosh Mehdizadeh[*1], Abbasali Sadeghi[2], Amirreza Sadeghi[3], Mohammad Hossein Razmkhah[4], Mohammad Yousef Nejati[5]

1. Department of Civil Engineering, Garmsar Branch, Islamic Azad University, Garmsar, Iran
2. Department of Civil Engineering, Mashhad Branch, Islamic Azad University, Mashhad, Iran
3. Department of Civil Engineering, University of Birjand, Birjand, Iran
4. Department of Civil Engineering, Semnan University, Semnan, Iran
5. Department of Civil Engineering, Faculty of Civil and Earth Resources, Central Tehran Branch, Islamic Azad University, Tehran, Iran
E-mail: Kourosh.mehdizadeh@iau.ac.ir; abbasali.sadeghi@mshdiau.ac.ir; amireza.sadeghi@birjand.ac.ir; razmkhah-m-h@semnan.ac.ir; nejatishayan1@gmail.com

Received: 13 March 2025; Accepted: 3 June 2025; Available online: 1 July 2025

Abstract: The seismic collapse of the building is a performance level in which the amount of human and financial damage reaches its maximum, so this event can be the most unfortunate accident in the construction industry. During strong earthquakes in different parts of the world, a more accurate assessment of the seismic collapse of structures and its prevention is one of the important challenges of structural engineers. In this way, any type of cut in the geometric or physical structure of the weld is called "discontinuity" when its value exceeds the specified limit. It is considered a "defect". There is a possibility of defects in the welding connections of steel structures. According to the seismic standards, the weld must be free of any defects and during an earthquake, weld failure should not occur. In this paper, the presence of defects in welding of beams-to-columns of the steel moment resisting frame (SMRF) connection is investigated for 4-story SMRF probabilistically by incremental dynamic analysis (IDA) and fragility curves under 7 far-fault earthquake records by two scenarios. Also, the influence of stiffness and strength deterioration is assumed according to the experimental results of the models. For this purpose, a normal distribution is used to consider the welding defect. Scenario I related to the removal of the connection of beam-to-column on the first story and scenario II was defined as the sudden removal of all the connections of the beams to columns of the first story. In the case of defects in welded connections, the results of this research showed that the important role of the quality of welding connection in seismic collapse capacity of structures. As an example, at the probability level of 50%, the seismic collapse capacity of the mentioned SMRF without defects in beam-to-column connection is 3.2g and the seismic collapse capacity of this SMRF has been obtained by applying probabilistic failure strains of 16%, 50% and 84% equal to 2.3g, 2.8g and 3.0g, respectively.
Keywords: Steel moment resisting frame (SMRF); Welding; Connection failure; Normal distribution; Failure strain.

1. Introduction

Steel connections are classified according to connection technology to riveted, bolted and welded joints. Seismic damage to the welded connections has been the main concern for structural engineers. Therefore, the research background is presented in the following. Wang et al. (2021) stated that the welding process always causes a loss of 40 to 60 times the fatigue strength of welded joints, which leads to relatively poor reliability during the service life of the connections [1]. When better performance is expected from the structure, the role of some factors such as reliability in welding is highlighted [2]. According to technical studies, the crack in the weld starts from the place where the stress is concentrated, as a result, the fracture in the weld is usually started from the toe of the welded metal, where the change in the weld surface geometry causes the stress to be concentrated [3-6]. The presence of slag, porosity, and microstructure heterogeneity are among the factors that cause welding failure [7-9]. Kim et al. (2018) showed that porosity greatly reduced the service life of weld compared to surface defects [10]. In short, it can be stated that defects caused by welding act as a source of failure and have a significant effect on the performance of the elements connected by welding [11]. Many studies have been done on steel moment resisting frame (SMRF) structures, which are described in the following. The behavior of SMRFs is investigated

under the collision of a vehicle to one of its columns by Sadeghi et al. (2022) using fragility curves [12] and Sadeghi et al. (2021) optimized the behavior of SMRFs under the effect of impact loadings by using evolutionary algorithms [13]. Saberi et al. (2021) compared the effect of progressive collapse on high-rise steel structures with different bracing systems [14]. Kouhestanian et al. (2021, 2023) conducted research on the effect of aftershocks as well as irregularity in the plan and height and investigated the amount of reduction in the capacity of the structure due to the presence of aftershocks, torsional irregularity in the plan and also the presence of a soft story [15, 16]. Saberi et al. (2022) investigated the effect of fire on steel structures. The findings of this research showed that by varying each of the factors, the damage modes are changed considering to the thickness of connections under thermal loadings [17]. Meng et al. (2023) studied the potential of progressive collapse occurrence in regular and irregular SMRFs with welded-flange bolted-web connections (WBCs) by considering the change of the bays [18]. Tarighi et al. (2023) investigated the behavior of SMRFs with repairable connections experimentally and numerically [19]. Sadeghi et al. (2024) investigated the impact of the pounding between two adjacent SMRFs consisting of 2 and 5 stories, characterized by intermediate ductility, while taking into account both equal and unequal heights during seismic excitations. The findings of the sensitivity analysis revealed that the yield strength of the cross-sections and the dead load had the most significant influence on the computation of failure probability. Furthermore, the results derived from the Kriging meta-model indicated that the failure probability increased by 65% when comparing unequal height frames to those of equal height [20]. Li et al. (2024) conducted a study on two methods for transverse strengthening—namely, the installation of diaphragms and the use of concrete-filled steel tube trusses (CFSTTs). A finite element model was created for a standard 30 m PCB bridge, which was validated against on-site load test results to ensure its reliability. The findings indicated that incorporating a transverse partition and CFSTTs significantly enhanced the load distribution of the PCB bridge and decreased the maximum deflection of the girder, particularly when the CFSTT reinforcement method was employed [21]. Mehdizadeh et al. (2025) evaluated the seismic collapse capacity of SMRFs that were designed using both the Equivalent Design (ED) and Performance-Based Plastic Design (PBPD) methodologies. The findings indicated that the seismic collapse capacities of frames designed with PBPD were markedly superior to those designed with ED, showing a 25% and 31% enhancement in collapse capacity for the five-story and ten-story frames, respectively, at a statistical significance level of 50% [22].

By reviewing the past technical studies, it was found that the incremental dynamic analysis (IDA) and fragility curves of SMRFs with weld defects have not been obtained so far. Therefore, in this study, the performance of a 4-story SMRF with two bays and rigid welded connections is evaluated by IDA and fragility curves. It is noted that the seismic collapse capacity of the mentioned model in the cases of sudden removal of the connection and application of welding defects is assessed in OpenSees software [23] under far-fault earthquake records probabilistically. Figure 1 presents the flowchart of current research for understanding the whole concepts of this paper.

2. Rigid beam-to-column welded connections in SMRF

Beams and columns in SMRFs are connected by joints so that they can easily bear gravity and lateral loads. In fact, connections have a great influence on the seismic behavior of SMRF structures. Steel beam-to-column connections are bolted and welded. After the earthquakes of Northridge (1997) and Kobe (1995), various studies have been conducted on welded joints and various recommendations have been made to strengthen all types of steel connections such as moment connection with top and bottom plates and saddle connection with vertical plates [24]. Mirghaderi and Dehghani (2008) evaluated the performance of moment saddle connections cyclically. The results of its research indicated the suitable performance to bear drift angles up to 0.08 rad without significantly reducing its strength that is an amount much larger than what is specified by the latest seismic standards [25]. Ghobadi et al. (2009) assessed five experimental samples of the flange plate connections with different details to develop suitable configurations to bear drift angles more than 0.05 rad [26].

3. Modeling verification

In this paper, for validating the modeling procedure, a 4-story SMRF structure with real dimensions is modeled in a 3-dimensional shaking table of E-Defense to evaluate the collapse performance of the aforementioned SMRF [27]. To apply the seismic load to the mentioned structure, the Kobe earthquake recorded at Takatori station was used, and the collapse of the structure was reported due to the sidesway collapse of the first floor. The list of cross-sections of beams and columns is mentioned according to Table 1. Also, Table 2 indicates the mechanical features of elements. Based on Figure 2, earthquakes at 4 acceleration levels of 20%, 40%, 60%, and 100% were applied to the mentioned structure, and the maximum story relative displacement ratio to story height of the structure was compared with the experimental outputs. Therefore, the results of the numerical modeling were in good agreement with the experimental ones.

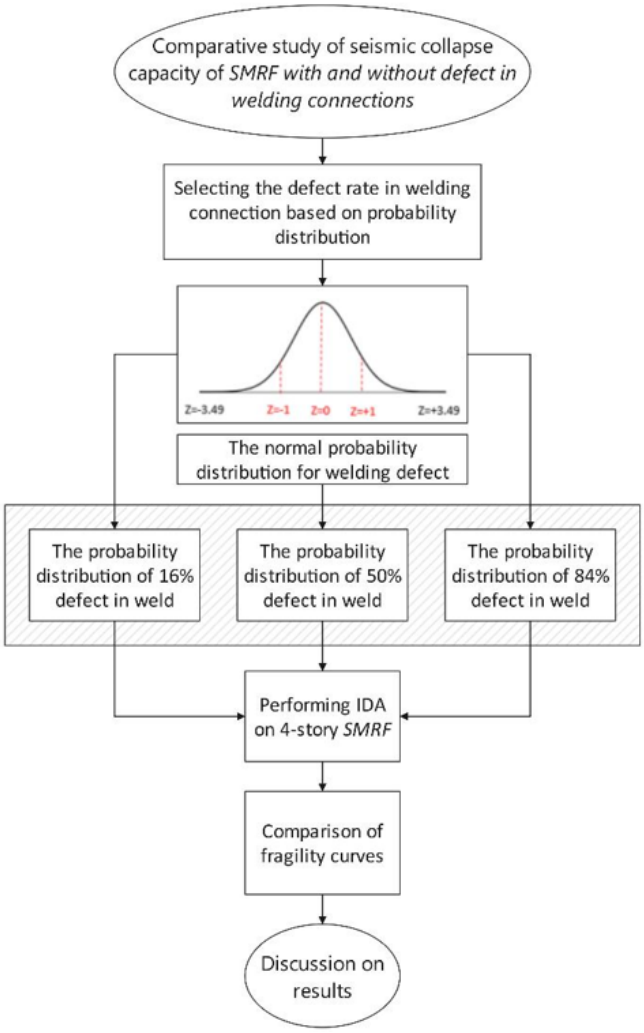

Figure 1. Flowchart of the current research.

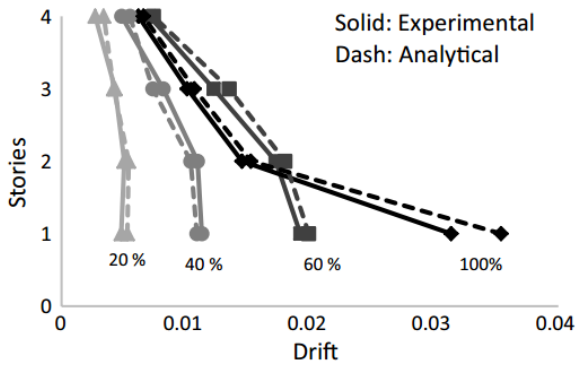

Figure 2. Comparison of drifts of numerical and experimental modeling at *4* acceleration levels.

Table 1. The cross-sections of beams and columns of the studied model [27].

Story	Column C1,C2(BCR295)	Story	Beam		
			G1(SN400B)	G11(SN400B)	G12(SN400B)
4	HSS300x9	4	H-346x174x6x9	H-346x174x6x9	H-346x174x6x9
3	HSS300x9	3	H-350x175x7x11	H-350x175x7x11	H-340x175x9x14
2	HSS300x9	2	H-396x199x7x11	H-400x200x8x13	H-400x200x8x13
1	HSS300x9	1	H-400x200x8x13	H-400x200x8x13	H-390x200x10x16

Table 2. The mechanical features of used materials [27].

Element	Used steel	Yield stress (MPa)	Tensile stress (MPa)
Beam	SN400B	235	400
Column	BCR295	295	400
Anchor bolt	SNR490B	325	490

4. Modeling process

In this research, the behavior and collapse capacity of verified experimental SMRF with 4-story with and without weld defect have been compared with each other probabilistically. The yield stress and tensile of the used steel and its elasticity modulus is 200000 MPa. Also, Steel01 model is considered for bilinear uniaxial steel materials with kinematic and isotropic stiffness according to a post-yielding stiffness of 3% [28]. In addition, the influence of stiffness and strength deterioration is assumed according to the experimental outputs. As a result, Ibarra-Medina-Krawinkler model (IMK) [29] is used for modeling the verified SMRF. In the following, Figure 3 shows the studied SMRF with the mentioned cross-sections of Table 1.

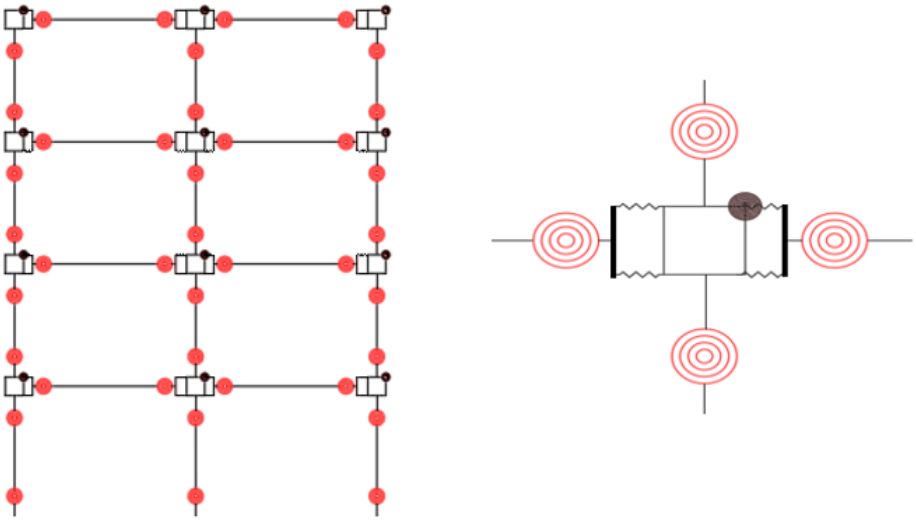

Figure 3. Simulation model of *OpenSees* software.

In this research, the modeling process of weld connections is presented based on the study of Soleimani and Behnamfar (2017) [24]. The behavior of this proposed pattern (moment-rotation) has better accuracy in modeling the beam-to-column connections versus other similar models in the past. This model expresses the connection behavior under positive and negative moments. This model can explain the behavior of different types of steel joints such as saddle connections. The proposed model of this research is a three-parameter model including the parameters of initial stiffness, post-elastic stiffness of the connection, which are indicated by parameters of K_i and K_p, respectively. Also, the parameter of M_0 is the moment base of the connection [24]. These parameters are shown schematically in Figure 4. The explanation of the parameters is presented in Reference [24].

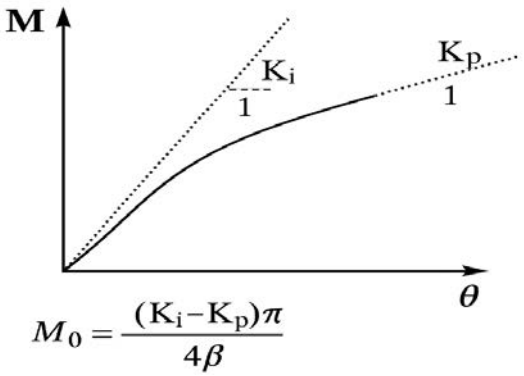

Figure 4. Proposed model of moment-rotation [24].

Based on the model proposed by Soleimani and Behnamfar (2017) [24], the stiffness of springs equivalent to welding the top and bottom plates to the column is presented based on Equations (1) and (2). The general pattern of the connection modeling is presented based on Figure 5.

$$K_1 = \frac{Et_t(b_2 - b_1)}{L_{t1}[1 - \left(\frac{b_2}{b_1}\right) - \ln\left(\frac{b_2}{b_1}\right)]} \quad (1)$$

$$K_2 = \frac{Eb_b t_b}{(b_b/2)} = 2Et_b \quad (2)$$

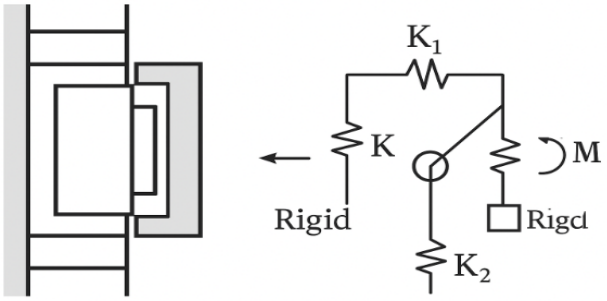

Figure 5. Proposed model of rigid connection [24].

The steel profiles utilized for modeling of SMRF are of the European standard ST37 and also, the welds are of E6013 electrode type. In the following, the stress-strain curve of ST37 for steel material of the beams and columns of the SMRF and the stress-strain curve of welding related to E6013 electrode are presented and elaborated in the Reference [24]. To take into account the possibility of defects in the implementation of the connection and especially the welding of the top and bottom plates to the column, fitting a normal distribution (or Log-Normal) to the failure strain of the springs equivalent to the welding of the mentioned plates have been used. Figure 6 shows the desired normal distributions to create probabilistic failure strains of these plates.

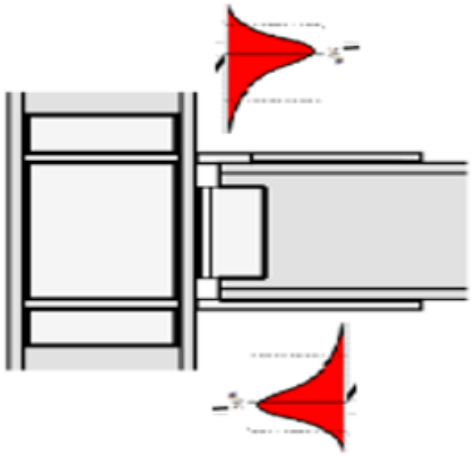

Figure 6. Illustration of the desired normal distributions to create the probabilistic stiffness of these plates.

In Figure 7, how to create a normal distribution to the failure strain of springs equivalent to rigid connection plates is shown. The mode of removing the connection or welding is considered equivalent to applying zero stiffness to the spring. Applying Z=+3.49 for behavior without connection defects and strain tolerance up to *0.23* capacity is proposed. To evaluate the probabilistic of the stiffness parameter, three probability levels representing the failure strains at three statistical levels of 16%, 50% and 84% (Z=-1, Z=0 and Z=+1) have been used.

One of the main problems in nonlinear dynamic analysis of structures is the selection of earthquakes and their number to obtain the results with appropriate accuracy. FEMA P 695 [30] suggests a set of near-fault and far-fault earthquake records for nonlinear dynamic analyses. In this research, IDA has been performed with small and controlled steps. According to FEMA P 695, to reduce the dispersion of the results, these records are first scaled

to the peak velocity of the accelerogram. Also, in the current research, the spectral acceleration of all records in the period of the first mode of the structure (S_a (T_1, 5%)) was scaled to one to reduce the dispersion of the results. In this study, IDA is performed and IDA curves are plotted. In the following, for calculating the seismic collapse capacity of SMRF with and without weld defect, fragility curves are obtained. Table 3 shows the features of the studied earthquakes.

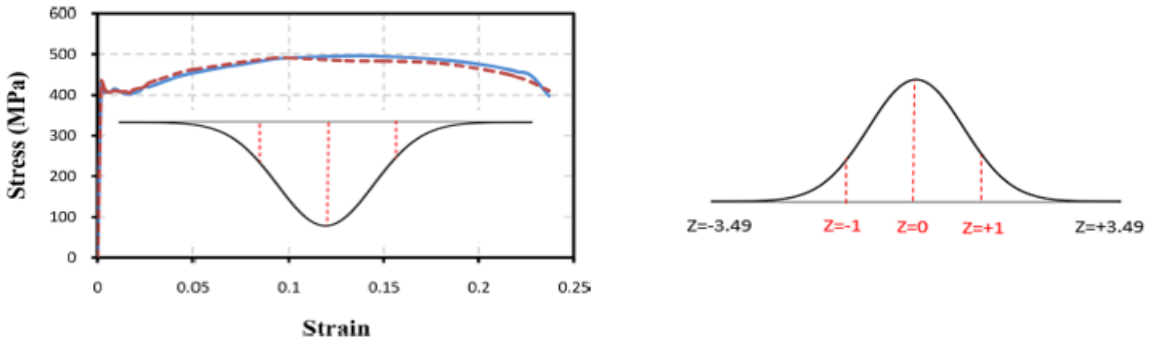

a) **b)**

Figure 7. How to fit the normal distribution to the weld failure strain of the connected plates to the top and bottom column.

Table 3. The features of the studied earthquakes.

ID No.	Date	Event	Station	Magnitude (M_w)	PGA[1] (g)	PGV[2] (cm/s^2)
1	1994	Northridge, CA	Beverly Hills-Mulhol	6.7	0.42	59
2	1994	Northridge, CA	Canyon Country-WLC	6.7	0.41	43
3	1999	Duzce, Turkey	Bolu	7.1	0.73	56
4	1999	Hector Mine, CA	Hector	7.1	0.27	29
5	1979	Imperial Valley, CA	Delta	6.5	0.24	26
6	1979	Imperial Valley, CA	El Centro Array # 11	6.5	0.36	35
7	1995	Kobe, Japan	Nishi-Akashi	6.9	0.50	37

[1] Peak ground acceleration
[2] Peak ground velocity

5. Results and discussion

According to Figure 8, initially, two scenarios of removing equivalent welding springs are considered. IDA has been carried out under 7 earthquakes that are mentioned in Section 4.1. Then the spectrum of earthquakes in the first vibration mode of the SMRF has been scaled to 1 and then their intensity has been increased by 0.1 in each step. In Figure 8, the dashed circles show the position of removing the equivalent springs of top and bottom welds at the beginning of the time history analyses in each step.

Figure 9 shows IDA curves of the desired SMRF under 7 far-fault earthquakes. The black graph is related to the main model. The gray graph corresponds to the results of the first scenario and the graph with low collapse capacity corresponds to the second scenario. These curves and results are related to the situation where it is assumed that at the very beginning of the earthquake, the welds of the top and bottom plates to the columns are failed. Figure 10 shows the collapse capacity by using fragility curves of the desired model in the states without defects and the scenarios defined in Figure 8. According to Figure 10, for example, at the probability level of 50%, the collapse capacity of the main model is 3.2g, the frame defined in the first scenario is 2.8g, and the frame corresponding to the second scenario is 0.9g. The first and second scenarios have reduced the SMRF collapse capacity by 12.5% and 71.8%, respectively. Similar interpretations can be made in other probability levels. As another interpretation, based on Figure 10, for example, for spectral acceleration of 3g, the collapse probability of the main model is 32%, the frame corresponding to the first and second scenarios is 58%, and 100%.

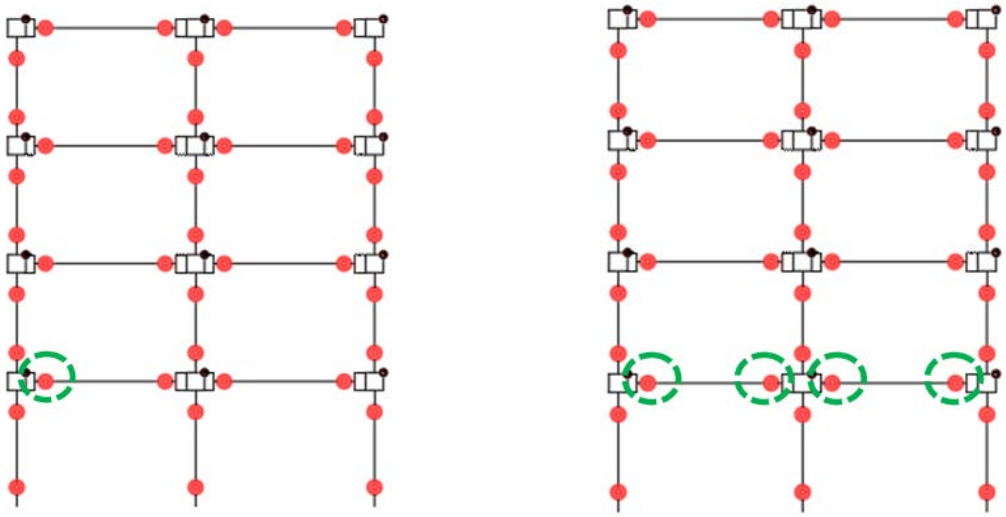

a) Spring Removal: K=0.0 Scenario I

b) Spring Removal: K=0.0 Scenario II

Figure 8. Two scenarios of removing weld-equivalent springs at the beginning of time history analyses.

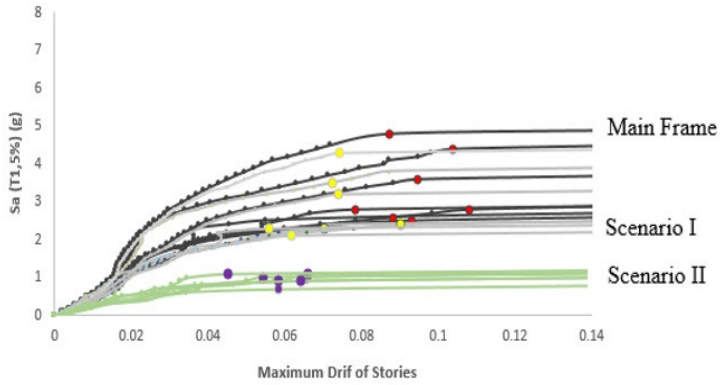

Figure 9. IDA curves of the desired SMRF in 3 cases, without defects in the implementation of connections, the first and second scenarios.

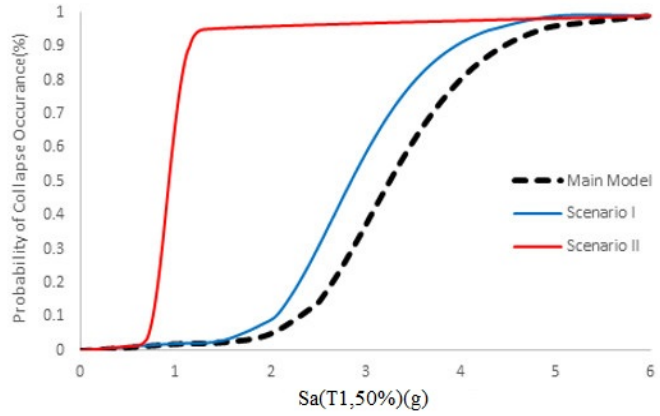

Figure 10. Fragility curves of the desired SMRF in 3 cases, without defects in the implementation of connections, the first and second scenarios.

By applying probabilistic strain to the behavior of defined springs equivalent to the welding of top and bottom plates in all beam-to-column connections of the desired frame, a structure with performance defects has been created in all connections. Figure 11 shows the deformed structure at 9.1 seconds and 19.6 seconds of the Duzce

earthquake. It is noted that these deformations are related to the failure strain of statistical level of 16% and an earthquake with an intensity of 1.8 times to the main earthquake.

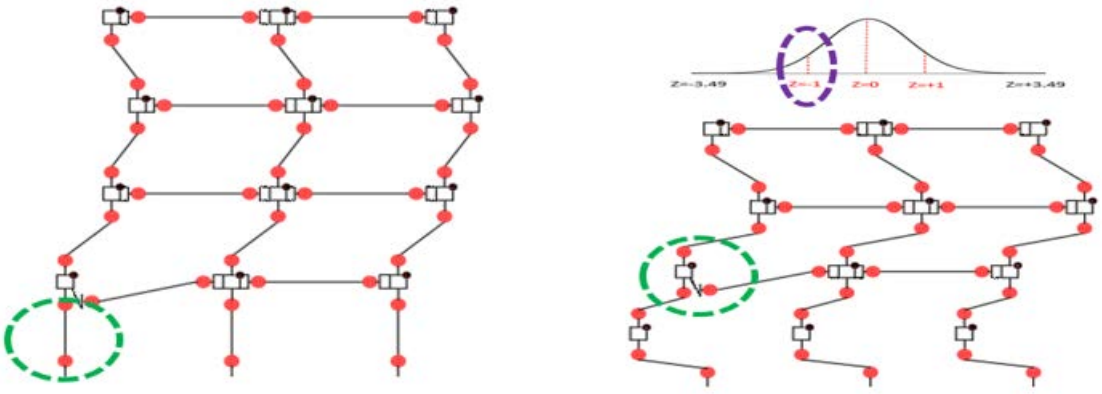

T=9.1 sec T=19.6 sec

Figure 11. Deformed model at 9.1 seconds and 19.6 seconds of Duzce earthquake with intensity 1.8 times that of the main earthquake.

Figure 12 shows the fragility curves of the collapse capacity of the main model without defects in the implementation of connections and SMRF with failure strain of 16%, 50%, and 84% based on the proposed normal distribution. Based on Figure 12, different possible interpretations can be presented for the collapse capacity of the studied SMRFs. For example, at the statistical level of 50%, the collapse probability of the main model is 3.2g. The seismic collapse capacity of the SMRF with applying the failure strains of 16%, 50%, and 84% is equivalent to 2.3g, 2.8g, and 3.0g, respectively.

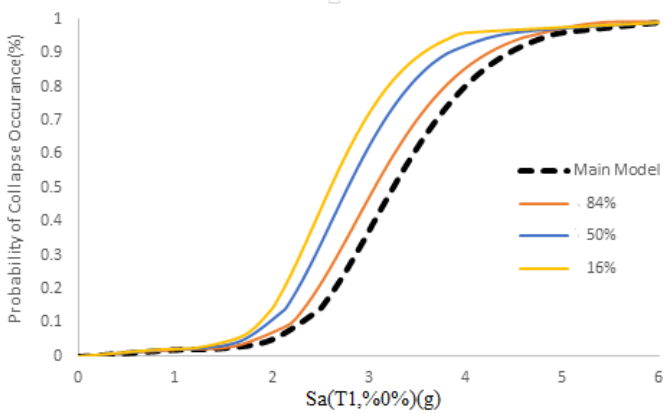

Figure 12. Fragility curves of the main model and SMRF with failure strain of 16%, 50%, and 84%.

6. Conclusions

In this research, the behavior of the 4-story SMRF is evaluated by considering the weld defect. In this way, by using the proposed models of the behavior of rigid welded joints, in the cases of sudden connection removal and welding defects, the seismic collapse capacity has been investigated probabilistically by performing IDA and plotting fragility curves. The main results of this research are highlighted in the following:

1) At the probability level of 50%, the collapse capacity of the main model is 3.2g, the frame defined in the first scenario is 2.8g, and the frame corresponding to the second scenario is 0.9g, and the first and second scenarios are reduced 12.5%, and 71.8% of the collapse capacity versus main model, respectively and for the spectral acceleration of 3g, the collapse probability of the main model, the first and second scenarios is 32%, 58%, and 100, respectively.

2) At the probability level of 50%, the collapse probability of the main model is 3.2g and the collapse capacity of the SMRFs with the application of 16%, 50%, and 84% failure strains is equivalent to 2.3g, 2.8g, and 3.0g, respectively. Also, as an example, for spectral acceleration of 3g, the collapse probability of the main model and SMRFs with failure strain of 16%, 50%, and 84% are 32%, 79%, 67% and 54%, respectively.

3) According to the obtained results, the defect of welding of connections can significantly increase the damage

potential in SMRF structures. For example, if amateur welders make a mistake in welding the beam-to-column connections of the first story (two defined scenarios), at a probability level of 50%, this shortcoming can reduce the collapse capacity in Scenarios I and II by 12.5%, and 71%, respectively.

6.1 Limitations

Despite the comprehensive analysis conducted in this study, several limitations should be acknowledged:

1) Simplified Modeling of Welding Defects: The welding defects were modeled using idealized geometric representations, which may not fully capture the complexity and variability of real-life welding flaws observed in practice.

2) Limited Range of Defect Types and Locations: Only a few common types of welding defects (e.g., lack of fusion, incomplete penetration, and porosity) were considered, and their locations were predefined at critical joints. Other possible defect scenarios and random spatial distributions were not investigated.

3) Assumptions in Material and Connection Behavior: The study assumed isotropic material properties and typical nonlinear behavior for steel and welds. Effects such as residual stresses, heat-affected zones (HAZ), and strain rate sensitivity during seismic loading were not explicitly modeled.

4) Fixed Frame Geometry: The investigation was limited to a specific steel moment-resisting frame configuration. Results may vary for frames with different geometries, story numbers, or load distributions.

5) Neglecting Cumulative Damage and Post-Earthquake Reparability: The analysis focused on collapse capacity without considering cumulative damage under multiple seismic events or the practicality of repairing the affected joints.

6.2 Future Work

To address the above limitations and enhance the understanding of welding defects in seismic performance, the following research directions are suggested:

1) Incorporation of Probabilistic Defect Modeling**:** Future studies could use probabilistic approaches to account for the uncertainty in the size, type, and location of welding defects, allowing for a more realistic assessment of risk.

2) Experimental Validation**:** Laboratory testing of steel joints with controlled welding defects under cyclic loading could validate the numerical models and provide better calibration for fracture and failure criteria.

3) Evaluation of Various Frame Typologies**:** Extending the study to different structural systems, including taller buildings or dual systems, could determine whether similar effects of welding defects are observed across other configurations.

4) Post-Earthquake Assessment and Repair Strategies**:** Exploring how welding defects affect the residual capacity of structures after an earthquake and developing practical repair guidelines for damaged connections.

7. References

[1] Wang D, Yao D, Gao Z, Wang Q, Zhang Z, Li X. Fatigue mechanism of medium-carbon steel welded joint: Competitive impacts of various defects. International Journal of Fatigue. 2021;151:106363.

[2] Knysh V, Solovei S, Osadchuk S, Nyrkova L. Influence of hardening by high-frequency mechanical impacts of butt welded joints made of 15KhSND steel on their atmospheric corrosion and fatigue fracture resistance. Materials Science. 2018;54:421–429.

[3] Radaj D, Sonsino C, Fricke W. Recent developments in local concepts of fatigue assessment of welded joints. International Journal of Fatigue. 2009;31(1):2–11.

[4] Radaj D. Review of fatigue strength assessment of nonwelded and welded structures based on local parameters. International Journal of Fatigue. 1996;18(3):153–170.

[5] Maddox S. Review of fatigue assessment procedures for welded aluminium structures. International Journal of Fatigue. 2003;25(12):1359–1378.

[6] Hobbacher A. The new IIW recommendations for fatigue assessment of welded joints and components–A comprehensive code recently updated. International Journal of Fatigue. 2009;31(1):50–58.

[7] Yamamoto H, Danno Y, Ito K, Mikami Y, Fujii H. Weld toe modification using spherical-tip WC tool FSP in fatigue strength improvement of high-strength low-alloy steel joints. Materials & Design. 2018;160:1019–1028.

[8] Lah NAC, Ali A, Ismail N, Chai LP, Mohamed AA. The effect of controlled shot peening on fusion welded joints. Materials & Design. 2010;31(1):312–324.

[9] Fu Z, Ji B, Kong X, Chen X. Grinding treatment effect on rib-to-roof weld fatigue performance of steel bridge decks. Journal of Constructional Steel Research. 2017;129:163–170.

[10] Kim DY, et al. Effect of porosity on the fatigue behavior of gas metal arc welding lap fillet joint in GA 590 MPa steel sheets. Metals. 2018;8(4):241.

[11] Hatamleh O, Hill M, Forth S, Garcia D. Fatigue crack growth performance of peened friction stir welded 2195 aluminum alloy joints at elevated and cryogenic temperatures. Materials Science and Engineering A. 2009;519(1–2):61–69.
[12] Sadeghi A, Kazemi H, Mehdizadeh K, Jadali F. Fragility analysis of steel moment-resisting frames subjected to impact actions. Journal of Building Pathology and Rehabilitation. 2022;7(1):26.
[13] Sadeghi A, Kazemi H, Samadi M. Single and multi-objective optimization of steel moment-resisting frame buildings under vehicle impact using evolutionary algorithms. Journal of Building Pathology and Rehabilitation. 2021;6:1–13.
[14] Saberi H, Saberi V, Sadeghi A, Pooyasefat A, Noroozinejad Farsangi E. Investigation of the occurrence of progressive collapse in high-rise steel buildings with different braced configurations. 2021.
[15] Kouhestanian H, Razmkhah MH, Shafaei J, Pahlavan H, Shamekhi Amiri M. Probabilistic evaluation of seismic performance of steel buildings with torsional irregularities in plan and soft story under mainshock-aftershock sequence. Shock and Vibration. 2023;2023.
[16] Razmkhah MH, Kouhestanian H, Shafaei J, Pahlavan H, Shamekhi Amiri M. Probabilistic seismic assessment of moment resisting steel buildings considering soft-story and torsional irregularities. International Journal of Engineering. 2021;34(11):2476–2493.
[17] Saberi H, Saberi V, Khodamoradi N, Pouraminian M, Sadeghi A. Effect of detailing on performance of steel T-connection under fire loading. Journal of Building Pathology and Rehabilitation. 2022;7(1):7.
[18] Meng B, Xiong Y, Zhong W, Li C, Li H. Collapse resistance analysis of steel frame structures with varying spans using component models. Structures. 2023;57.
[19] Tarighi P, Kafi MA, Vahdani R. Experimental and numerical investigation of the performance of replaceable-rigid connection. Structures. 2023;53:12–28.
[20] Sadeghi A, Kazemi H, Razmkhah MH, Sadeghi A. Probabilistic investigation of the pounding effect in steel moment resisting frames with equal and unequal heights. Research in Engineering Structures and Materials. 2024;10(4):1431–1449.
[21] Li P, Yang C, Xu F, Li J, Jin D. Reinforcement of insufficient transverse connectivity in prestressed concrete box girder bridges using concrete-filled steel tube trusses and diaphragms: A comparative study. Buildings. 2024;14(8):2466.
[22] Mehdizadeh K, Sadeghi A, Sadeghi A, Razmkhah MH. Evaluation of the seismic collapse capacity of steel moment-resisting frames designed using elastic design (ED) and performance-based plastic design (PBPD) methodologies. I-manager's Journal on Civil Engineering. 2025;15(1):1–12.
[23] OpenSees. Open system for earthquake engineering simulation manual. Pacific Earthquake Engineering Research Center, University of California, Berkeley. 2007. http://opensees.berkeley.edu.
[24] Soleimani E, Behnamfar F. New moment-rotation equation for welded steel beam-to-column connections. International Journal of Steel Structures. 2017;17:389–411.
[25] Mirghaderi SR, Dehghani Renani M. The rigid seismic connection of continuous beams to column. Journal of Constructional Steel Research. 2008;64(12):1516–1529.
[26] Ghobadi MS, Mazroi A, Ghassemieh M. Cyclic response characteristics of retrofitted moment resisting connections. Journal of Constructional Steel Research. 2009;65(3):586–598.
[27] Suita K, Yamada S, Tada M, Kasai K, Matsuoka Y, Sato E. E-defense tests on full-scale steel buildings: Part 2—Collapse experiments on moment frames. In: Proceedings of Structures Congress, ASCE, Long Beach. 2007:247–18.
[28] Kim J, Park J, Lee T. Sensitivity analysis of steel buildings subjected to column loss. Engineering Structures. 2011;33:421–432.
[29] Ibarra LF, Medina RA, Krawinkler H. Hysteretic models that incorporate strength and stiffness deterioration. Earthquake Engineering and Structural Dynamics. 2005;34(12):1489–1511.
[30] FEMA P695. Quantification of building seismic performance factors. Federal Emergency Management Agency, Washington, DC, USA. 2009.